JOURNAL OF GEOPHYSICAL RESEARCH, VOL. 106, NO. C3, PAGES 4655–4664, MARCH 15, 2001

Improved electromagnetic bias theory: Inclusion of hydrodynamic modulations

T. Elfouhaily and D. R. Thompson

Applied Physics Laboratory, The Johns Hopkins University, Laurel, Maryland

B. Chapron

Département d'Océanographie Spatiale, Institut Français de Recherche pour l'Exploitation de la Mer
Brest, France

D. Vandemark

Laboratory for Hydrospheric Processes, NASA Goddard Space Flight Center, Wallops Island, Virginia

Abstract. The modulation of short ocean waves by longer ones is a likely contributor to the radar altimeter's electromagnetic ranging bias (EM bias). An analytic model to account for this component of the EM bias is developed here under a two-scale two-dimensional hydrodynamic assumption. Following the principle of wave action balance, a standard hydrodynamic modulation transfer function is used to establish that the longer modulating waves enter the EM bias formulation not only through their elevation and slope variables but also through their quadratures. These latter contributions help to explain the role of long-wave slope and orbital velocity fields within the EM bias problem. Simplified analytical expressions are derived using linear Gaussian statistics for both modulating and modulated waves. For the sake of completeness an outline of the possible extension to nonlinear interacting waves is provided.

1. Introduction and Issues

In a recent work [*Elfouhaily et al.*, 2000] the electromagnetic bias theory of *Srokosz* [1986] has been extended by using a two-scale surface model that includes the tilting of short waves caused by long waves. Short-wave statistics involved in the computations were held constant within each tilted patch regardless of the overall variation of the underlying long waves. It was shown that the added effect of tilting changes the previous theory considerably. The impact on the electromagnetic ranging bias (EM bias) was found to be as high as 50% and directly related to the strength of the ratios between short- and long-wave slope variances. These ratios entered the tilt EM bias as arguments of complicated functions that have simplified forms only under special cases. Those new functions were termed the weighting functions.

Rodriguez et al. [1992] pointed out that correlation between the nadir-viewing radar cross section and the surface elevation may also come from variation of local short-wave statistics over the phase of long waves. In that numerical study a Monte Carlo simulation was used, including a modulation transfer function, to make a first attempt at assessing this component of the EM bias. This numerical experiment, elaborated by *Rodriguez et al*. [1992], has several shortcomings, among them a one-dimensional representation of an inherently two-dimensional problem. However, that study has had a major impact on identifying the significant role played by short waves in the explanation of measured EM biases. To date, no analytical theory has been developed to predict a range bias due to this induced nonlinearity in short waves (modulated waves) that is caused by the underlying long waves (modulating waves), be they linear or nonlinear.

In this paper our goal is to provide a rational mathematical formulation for the EM bias when hydrodynamic modulations are considered. First, we identify and define the hydrodynamic EM bias to distinguish it clearly from tilt-induced effects [*Elfouhaily et al*., 2000]. Following a standard modulation transfer function model, we assume that the surface wave spectrum may be divided into two parts to distinguish the narrow-band fast moving "long waves" from the shorter modulated wave components. The principle of wave action balance can then describe the interactions between these long and short surface waves. As developed hereafter, modulation of the short-wave statistical moments are expressed as function of a six-dimensional (6-D) vector, whose components are determined by the elevation and slopes of long waves as well as their quadratures (also known as Hilbert transformed). The corresponding 6-D joint probability density function (PDF) is then developed under a Gaussian assumption to provide a convenient analytical formulation. Finally, this formalism is extended to include non-Gaussian statistical descriptions for both short and long wave PDFs.

2. Definition of the EM Bias Due to Hydrodynamic Interactions

By common definition the altimeter EM bias is the normalized correlation between the radar cross section (σ^o) and the long-wave elevation (ζ). Variations in the radar cross section are partially caused by long-wave tilts. If local short-wave statistics are assumed to be constant, then this variation is termed tilt modulation. The hydrodynamic modulation, however, implies variation in the short-wave statistics along the phase of long waves.

Paper number 1999JC000086.
0148-0227/01/1999JC000086$09.00

The relative cross correlation can then be explicitly written as

$$\beta_{EM} = \frac{\langle \zeta \tilde{\sigma}^o \rangle}{\langle \sigma^o \rangle} = \frac{\langle \zeta(\sigma^o + \delta\sigma^o) \rangle}{\langle \sigma^o \rangle} = \frac{\langle \zeta\sigma^o \rangle}{\langle \sigma^o \rangle} + \frac{\langle \zeta\delta\sigma^o \rangle}{\langle \sigma^o \rangle} \overset{\Delta}{\equiv} \beta_T + \beta_H, \quad (1)$$

where β_T and β_H are identified as biases due to tilt and hydrodynamic modulation, respectively. As understood, the tilt bias will exist only under the condition of nonlinear long-wave statistics. If the long modulating waves are linear, the tilt bias is zero. Any tilt bias can be decomposed further into two biases. First-order tilt bias is a function of the cross skewness between surface elevation and slopes as well as ratios of the slope variances. The second-order tilt bias involves high-order statistics such as the cross kurtosis between elevation and slopes, but as shown by *Elfouhaily et al*. [2000], this "second-order" effect can impact results by nearly 50%.

In the same manner the hydrodynamic component β_H can be separated into two identifiable terms. The first is due to direct modulation of linear short waves by linear long waves. The induced nonlinearity caused by the hydrodynamic modulation generates an EM bias even though the interacting waves were originally linear. This phenomenon makes the hydrodynamic bias fundamentally different from the tilt bias. In sections 3–6 we develop this first-order hydrodynamic term. In section 7, nonlinear waves will be assumed to develop the second type of this hydrodynamic bias, which will justify and ensure the parallel with the second-order tilt bias developed by *Elfouhaily et al*. [2000]. We now investigate σ^o and its relation to the short-wave statistics to assess its relative variation when short waves are modulated hydrodynamically.

3. Modulation of the Radar Cross Section

Under the Geometric Optics (GO) assumption [e.g., *Barrick*, 1968] the ocean surface's radar cross section at nadir incidence is proportional to the short-wave PDF $P_s(\mathbf{x}_L)$ multiplied by the geometric correction $T(\mathbf{x}_L)$ of the local tilt angle,

$$\sigma^o \propto 2\pi T(\mathbf{x}_L) P_s(\mathbf{x}_L) \overset{\Delta}{\equiv} 2\pi(1 + {}^t\mathbf{x}_L\mathbf{x}_L)^2 \frac{1}{2\pi\sqrt{d_s}} e^{-1/2\,{}^t\mathbf{x}_L\mathbf{V}_s^{-1}\mathbf{x}_L}, \quad (2)$$

where the surface slope vector and the covariance matrix of short waves are defined as

$$\mathbf{x}_L = \begin{pmatrix} \zeta_x \\ \zeta_y \end{pmatrix}, \ \mathbf{V}_s = \begin{pmatrix} \kappa_{20} & \kappa_{11} \\ \kappa_{11} & \kappa_{02} \end{pmatrix}. \quad (3)$$

The variable d_s is the determinant of the covariance matrix V_s,

$$d_s = |\mathbf{V}_s| = \kappa_{20}\kappa_{02} - \kappa_{11}^2. \quad (4)$$

The leading superscript t represents the algebraic transpose of a vector or a matrix, a notation used throughout this paper. The surface slope vector is, under geometric optics, the ratio between the horizontal and the vertical components of the incident electromagnetic wavenumber. In (2) the PDF of short waves is assumed to be Gaussian to help simplify the analytic relationship between the EM bias and the hydrodynamic modulation.

From (2) and (3), σ^o depends on the slope variances of short waves in two orthogonal directions (κ_{20} and κ_{02}) as well as on the cross correlation between the slope components (κ_{11}). A relative variation in σ^o can be readily expressed as a sum of relative variations of each of the slope moments. These slope moments enter the σ^o expression through the short-wave PDF; see (2). This relative variation is

$$\frac{\delta\sigma^o}{\sigma^o} = f_{20}\frac{\delta\kappa_{20}}{\kappa_{20}} + f_{11}\frac{\delta\kappa_{11}}{\kappa_{11}} + f_{02}\frac{\delta\kappa_{02}}{\kappa_{02}}, \quad (5)$$

where the f functions are given in Appendix A. The next challenge is to write the variation of short-wave statistics in terms of the hydrodynamic modulation.

4. Hydrodynamic Modulation

The strength of the hydrodynamic modulation theory lies in a linearization of the wave action balance equation. This linearization yields a simple notation based on what is called the modulation transfer function (MTF) of the hydrodynamic interactions. *Alpers and Hasselmann* [1978] were the first to express the MTF in the Fourier domain as a function of both long and short wavenumbers.

4.1. Formulation and Definitions

The relative modulation of the wave spectrum can be written in the Fourier domain as

$$\frac{\delta\Psi}{\Psi_e} = \int R(\mathbf{k}_L, \mathbf{k}_s) Z_{\mathbf{k}_L} e^{-1(\mathbf{k}_L\cdot\mathbf{r} - \omega_L t)}\, d\mathbf{k}_L + c.c., \quad (6)$$

where $R(\mathbf{k}_L, \mathbf{k}_s)$ is the modulation transfer function and $Z_{\mathbf{k}_L}$ is the Fourier transform of the elevation of long modulating waves,

$$\zeta(\mathbf{r}, t) = \int Z_{\mathbf{k}_L} e^{-1(\mathbf{k}_L\cdot\mathbf{r} - \omega_L t)}\, d\mathbf{k}_L. + c.c. \quad (7)$$

The symbol $c.c.$ means that the complex conjugate is added to guarantee a result that is real.

4.2. Modulation Transfer Function Concept

This first paper of *Alpers and Hasselmann* [1978] contained many typographical errors and assumed an inconvenient convention for the phase of the modulation. For this reason we rederive their MTF in its most general form. The linearization of the wave action balance equation is retained. However, we further include an additional term in the MTF because of the local acceleration inflicted on the short waves by the modulating waves. The corrected two-dimensional MTF can be written in a compact form as follows:

$$R(\mathbf{k}_L, \mathbf{k}_s) = (c_s\mathbf{k}_L \cdot \mathbf{k}_s + L_g)(\mathbf{k}_L \cdot \mathbf{\Pi}_s) M_L^s, \quad (8)$$

where c_s is the phase speed of short waves and L_g is the additional term generated by the effective acceleration of gravity, written explicitly as

$$L_g = -\tfrac{1}{2} k_L \omega_L. \quad (9)$$

If L_g is neglected in (8), the MTF would be identical to the original one by *Alpers and Hasselmann* [1978] (with the exception of the typos). The extra correction L_g is omnidirectional, which means it has the same strength regardless of the relative orientation of the modulating and modulated waves. For this reason the effect of local gravity seems to be more important when long and short waves are mutually orthogonal. Because of the presence of L_g, our modified MTF is not zero as in the original formulation by *Alpers and Hasselmann* [1978]. The magnitude of L_g in (9) runs from 1 to 10% of the MTF when both long and short waves are aligned according to our calculations. Also in (8), M_L^s is a complex function combining both short and long waves, and the vector $\mathbf{\Pi}_s$ is defined in terms of the gradient of the equilibrium spectrum of short waves. Their expressions are given by

$$M_L^s = -\frac{\omega_L + i\mu_s}{\omega_L^2 + \mu_s^2}\frac{c_L}{c_s} \tag{10a}$$

$$\mathbf{\Pi}_s = \frac{1}{\Psi_e}\nabla\Psi_e(\mathbf{k}_s) - \gamma_s\frac{\mathbf{k}_s}{k_s^2}, \tag{10b}$$

where μ_s is the relaxation rate of short waves. We note that μ_s, incorrectly, is often assumed in hydrodynamic studies to be equal to the growth rate β_s. *Kudryavtsev* [1994] explicitly showed that the ratio ρ between the relaxation rate and the growth rate is related to the exponent of the friction velocity u^* in the equilibrium spectrum Ψ_e relative to that in the growth rate β_s:

$$\rho \overset{\Delta}{\equiv} \left(\frac{\partial \ln \beta_s}{\partial u^*}\right)\left(\frac{\partial \ln \Psi_e}{\partial u^*}\right)^{-1}. \tag{11}$$

When using the unified equilibrium spectrum by *Elfouhaily et al*. [1997] and the growth rate given by *Plant* [1982] in (11), one gets

$$\rho = \begin{cases} 2\left(1 + \ln\dfrac{u^*}{c_m}\right) & u^* \le c_m, \\ 2\left(1 + 3\ln\dfrac{u^*}{c_m}\right) & u^* \ge c_m, \end{cases} \tag{12}$$

where c_m is the minimum phase speed. The most likely value of this ratio is 2 when u^* equals c_m, which corresponds to the most probable wind of 7 m s^{-1} on the oceans. A value of 2 for the ratio is consistent with *Phillips* [1985] and produces whitecapping coverage proportional to u^{*3}.

It must be noted at this point that the ratio ρ is not a free parameter and it is seldom equal to 1, contrary to common practice. As outlined above, the choice of the couplet equilibrium spectrum and growth rate determines the form of the ratio as a function of the wind speed or even wavenumber. For instance, if the chosen equilibrium spectrum has a linear dependence on the friction velocity, the relaxation rate must be twice as large as Plant's growth rate. If, however, the dependence behaves more as a square root of the friction velocity, then μ_s becomes 4 times larger than the growth rate β_s.

4.3. Limited Scope of the MTF

If we look more closely at the MTF in (8), we immediately notice the highly nonlinear dependence on the wavenumber of the modulating waves. Indeed, if one were to expand the MTF in (8) into powers of $\mathbf{k}_L$, one would find an infinite series. The implication of high powers in $\mathbf{k}_L$ are clear when the MTF is introduced back into (6). The infinite series in powers of $\mathbf{k}_L$ in the MTF will solicit an unlimited contribution from the modulating waves through its higher-order derivatives. In other words the nonlinear dependence of the MTF on $\mathbf{k}_L$ would require knowledge of all moments of the long waves. Hence elevation and slopes are not sufficient, and curvature and higher-order derivatives are required implicitly by (6). The theoretical basis for this involvement is sound and reasonable when the long modulating waves are linear. In this case the higher-order moments could be considered as redundant information since the linear elevation would already fully determine the surface.

In real-world situations, however, modulating waves are not linear. Assumed spectra (or direct measurements) are usually used to quantify the contribution of the modulating waves. In reality, higher-order moments of the surface cannot be fully determined. For instance, a spectrum can provide accurate information on modulating waves up to the slope moments. Measurements can only be trusted up to the first few moments. There is no reliable theoretical spectrum or in situ measurements that can provide reasonable estimates for all higher-order surface moments. For these reasons we suggest that the MTF in (8) be expanded only in powers of $\mathbf{k}_L$ about $\mathbf{k}_q$ ($\mathbf{k}_p \le \mathbf{k}_q \le \mathbf{k}_s$), where $\mathbf{k}_p$ is the wavenumber of the dominant spectral peak and $\mathbf{k}_s = \alpha\mathbf{k}_p$ is the separation scale between long and short waves. This separation is based on the concept of a narrow-band process [see *Tayfun*, 1986] modulating a broader-band process comprised of short waves. The multiplicative factor α must be smaller than 30, which is determined by the narrow-band criterion defined by *Longuet-Higgins* [1975]. This criterion ν_k is based on spectral moments, see *Longuet-Higgins* [1975] for definition, and must be less then unity to guarantee that long waves obey the narrow-band property. A value of 10 for α corresponds to 0.74 for ν_k. Knowing that the criterion in wavenumber is approximately twice that of frequency, we conclude that $\nu_\omega \approx \nu_k/2 = 0.37$ is comparable to values given by *Longuet-Higgins* [1975] and *Liu* [1976]. We note that $\alpha = 10$ was already used by *Donelan and Pierson* [1987] and *Elfouhaily et al*. [1997] as an intrinsic scale separation in their surface wave spectra.

The Taylor expansion of the MTF in (8) is

$$R(\mathbf{k}_L, \mathbf{k}_s) = R_q(\mathbf{k}_s) + \nabla R_q \cdot (\mathbf{k}_L - \mathbf{k}_q) \tag{13}$$

up to the linear order in $\mathbf{k}_L$, which is the smallness parameter in this expansion. The expansion is truncated at the first linear order and because the spectrum of long waves is narrow-banded and will be sufficient for elevation and slope moments only. R_q is simply the evaluation of the MTF at the wavenumber $\mathbf{k}_q$, and ∇R_q is defined and provided in Appendix B.

5. Implication of the Modulation

The hydrodynamic MTF formulated in section 4 is now used as a tool to express the modulated spectrum from which a direct link can be made to the modulated moments.

5.1. Modulated Spectrum

The Taylor expansion of the MTF in (13) leads to a simplified modulated spectrum when introduced in (6). Namely, the constant term of the expansion $R_q(\mathbf{k}_s)$ will relate the modulation to the surface elevation and its quadrature. Similarly, the factor ∇R_q will yield slope components and their quadratures. The expression for the modulated spectrum becomes

$$\begin{aligned}\frac{\delta\Psi}{\Psi_e} &= (a_q\cos\phi_q - a_\Delta\cos\phi_\Delta)\zeta + a_x\sin\phi_x\zeta_x + a_y\sin\phi_y\zeta_y \\ &\quad + (a_q\sin\phi_q - a_\Delta\sin\phi_\Delta)\check{\zeta} - a_x\cos\phi_x\check{\zeta}_x \\ &\quad - a_y\cos\phi_y\check{\zeta}_y \overset{\Delta}{\equiv} \mathbf{C}_{\mathbf{k}_s}\cdot\mathbf{u}_L,\end{aligned} \tag{14}$$

which is a dot product between two 6-D vectors. Here a and ϕ are amplitude and phase, respectively, of the quantities referred to in the subscripts and explained below in (16). $\mathbf{C}_{\mathbf{k}_s}$ is a function of short waves as defined through the formulation of the MTF, and $\mathbf{u}_L$ is the six-dimensional vector of long waves formed by the elevation and slopes as well as their quadratures (referred to with a breve over the variable):

$$^t\mathbf{u}_L \stackrel{\Delta}{\equiv} (\zeta,\ \zeta_x,\ \zeta_y,\ \breve{\zeta},\ \breve{\zeta}_x,\ \breve{\zeta}_y). \tag{15}$$

This 6-D vector will be called the moment vector throughout this paper. We must point out that the presence of the quadrature signals is essential in order to capture the phase of the modulation even though the process is totally formulated in the space and time domain instead of in the Fourier domain. The quadrature of a signal, symbolized by a breve over the variable name, implicitly refers to a 90° difference in the phases of the harmonics. More generally speaking, a quadrature of a signal is defined as its Hilbert transform.

The indices in (14) are abbreviations for the more complicated formulas as described by the relations

$$q \to R(\mathbf{k}_L,\ \mathbf{k}_s)|_{\mathbf{k}_L=\mathbf{k}_q}, \tag{16a}$$

$$\Delta \to \mathbf{k}_q \cdot \nabla R(\mathbf{k}_L,\ \mathbf{k}_s)|_{\mathbf{k}_L=\mathbf{k}_q}, \tag{16b}$$

$$x \to (\nabla R(\mathbf{k}_L,\ \mathbf{k}_s)|_{\mathbf{k}_L=\mathbf{k}_q})_x, \tag{16c}$$

$$y \to (\nabla R(\mathbf{k}_L,\ \mathbf{k}_s)|_{\mathbf{k}_L=\mathbf{k}_q})_y. \tag{16d}$$

These indices are applied to each amplitude a and phase ϕ of the complex quantities derived from the expansion of the hydrodynamic MTF.

5.2. Modulated Moments

Surface moments enter the radar cross-section expression under a GO approximation. Modulation of those moments can be computed from the modulated spectrum in (14) to give

$$\delta\kappa_{mn} = \mathbf{u}_L \cdot \iint (\mathbf{k}_s)_x^m (\mathbf{k}_s)_y^n \Psi(\mathbf{k}_s)\mathbf{C}_{\mathbf{k}_s}\, d\mathbf{k}_s \stackrel{\Delta}{\equiv} \mathbf{u}_L \cdot \mathbf{C}_{mn}, \tag{17}$$

which is, again, a dot product between two 6-D vectors, the moment vector $\mathbf{u}_L$ and the coupling vector $\mathbf{C}_{mn}$. A nice property of this formulation is that the modulated moments are linear functions of the moment vector $\mathbf{u}_L$.

Unfortunately, this linear dependence does not hold for the modulation of the radar cross-section itself even though it is again a dot product between two 6-D vectors. The relative modulation of σ^o is then

$$\frac{\delta\sigma^o}{\sigma^o} = \mathbf{u}_L \cdot \left(f_{20}\frac{\mathbf{C}_{20}}{\kappa_{20}} + f_{11}\frac{\mathbf{C}_{11}}{\kappa_{11}} + f_{02}\frac{\mathbf{C}_{02}}{\kappa_{02}} \right) \stackrel{\Delta}{\equiv} \mathbf{u}_L \cdot \Sigma(\mathbf{x}_L), \tag{18}$$

where the $\Sigma(\mathbf{x}_L)$ is the variable 6-D vector. The f functions are given in Appendix A.

5.3. Repercussion on the EM Bias

The effect of the hydrodynamic MTF on the EM bias becomes clear when (18) is used in the expression of the hydrodynamic bias in (1),

$$\beta_H = \frac{\langle \zeta\delta\sigma^o \rangle}{\langle \sigma^o \rangle} = \frac{\langle \zeta\sigma^o[\mathbf{u}_L \cdot \Sigma(\mathbf{x}_L)] \rangle}{\langle \sigma^o \rangle}$$

$$= \frac{\int \zeta\sigma^o[\mathbf{u}_L \cdot \Sigma(\mathbf{x}_L)]P_L(\mathbf{u}_L)\, d\mathbf{u}_L}{\int \sigma^o P_L\, d\mathbf{u}_L}, \tag{19}$$

where $P_L(\mathbf{u}_L)$ is the long-wave joint PDF. The value of the radar cross section σ^o in (2) can also be used to give

$$\beta_H = \frac{\int T(\mathbf{x}_L)[\mathbf{u}_L \cdot \hat{\mathbf{e}}_\zeta][\mathbf{u}_L \cdot \Sigma(\mathbf{x}_L)]P_s(\mathbf{x}_L)P_L(\mathbf{u}_L)\, d\mathbf{u}_L}{\int T(\mathbf{x}_L)P_s(\mathbf{x}_L)P_L(\mathbf{u}_L)\, d\mathbf{u}_L}, \tag{20}$$

where the identity $\zeta \equiv \mathbf{u}_L \cdot \hat{\mathbf{e}}_\zeta$ explicitly shows the dependence on the entire moment vector. Equation (20) is a general solution in the sense that it gives a good idea of how the hydrodynamic modulation is involved in the final expression of the hydrodynamic bias. Note that the numerator integrand in (20) is of even power in the moment vector. This observation turns out to be useful for the evaluation of the final analytical expression.

6. Analytical Evaluation of the Hydrodynamic Bias

In order to find a simple expression for the hydrodynamic bias the integrals in (20) must be evaluated. Since both PDFs, P_s and P_L, are assumed to be Gaussians, the multiplication will result in a combined multidimensional Gaussian. The resulting 6-D Gaussian is naturally coupled in all its six moments. The main coupling coefficients are the cross correlations between the two slope components. Another interesting coupling coefficient is the cross-correlation between the moments and their quadratures. Two successive changes of variables will be needed to decouple successfully the 6-D Gaussian for analytical evaluation.

To ease the development, we start with a Gaussian distribution for the long modulating waves. A more general distribution will replace this assumption in section 7. For this 6-D problem a Gaussian distribution can be written as

$$P_L(\mathbf{u}_L) = \frac{1}{(2\pi)^3\sqrt{|\mathbf{V}_L|}}\, \mathrm{e}^{-1/2\, ^t\mathbf{u}_L \mathbf{V}_L^{-1}\mathbf{u}_L}, \tag{21}$$

where $\underline{\underline{V}}_L$ is the cross-covariance matrix. Its description can be expressed in terms of two submatrices, $\underline{\underline{\alpha}}$ and $\underline{\underline{\beta}}$, as

$$\mathbf{V}_L = \begin{pmatrix} \boldsymbol{\alpha} & \boldsymbol{\beta} \\ ^t\boldsymbol{\beta} & \boldsymbol{\alpha} \end{pmatrix}. \tag{22}$$

This representation benefits from the fact that the covariance matrix is symmetric. Within the submatrix $\boldsymbol{\alpha}$ the statistics are restrained to either regular moments or to the quadrature moments. No cross correlation between signals and their quadratures is captured by this $\boldsymbol{\alpha}$ submatrix. On the other hand, $\boldsymbol{\beta}$ represents the possible correlation between the moments and their quadratures. The submatrices $\boldsymbol{\alpha}$ and $\boldsymbol{\beta}$ are defined as

$$\boldsymbol{\alpha} = \begin{pmatrix} \kappa_{200} & 0 & \\ 0 & \kappa_{020} & \kappa_{011} \\ 0 & \kappa_{011} & \kappa_{002} \end{pmatrix} \qquad \boldsymbol{\beta} = \begin{pmatrix} 0 & \kappa_{\breve{1}10} & \kappa_{10\breve{1}} \\ -\kappa_{\breve{1}10} & 0 & 0 \\ -\kappa_{10\breve{1}} & 0 & 0 \end{pmatrix}, \tag{23}$$

where the nonzero elements in $\boldsymbol{\beta}$ are simply

$$\kappa_{110} = -\kappa_{\breve{1}10} \stackrel{\Delta}{\equiv} \iint (\mathbf{k}_L)_x \Psi(\mathbf{k}_L)\, d\mathbf{k}_L \tag{24a}$$

$$\kappa_{101} = -\kappa_{10\bar{1}} \stackrel{\Delta}{\equiv} \iint (\mathbf{k}_L)_y \Psi(\mathbf{k}_L)\, d\mathbf{k}_L \tag{24b}$$

and the integration over the spectrum of long waves is defined in the same manner as for the regular moments. The latter elements can be interpreted as proportional to the variance of the orbital velocities of the modulating waves in either the x or the y direction. The proportionality constant between $\kappa_{10\bar{1}}$, $\kappa_{1\bar{1}0}$ and the orbital velocity variance is the acceleration of gravity g as in $k = \omega^2/g$.

6.1. First Change of Variable

In addition to a first change of variable, we will assume $\kappa_{011} = 0$ without loss of generality. Indeed, one can always choose the observation frame of reference to be aligned with the long modulating waves. However, one cannot assume alignment with short and long waves simultaneously without harming the generality of the problem.

The first change of variable needed is the normalization by the variance of each variable. We also include in this change of variable the determinant of the resulting matrix in order to simplify the expression of its inverse, which is used later in this development. Formally, the change of variable is

$$\mathbf{D}_L \stackrel{\Delta}{\equiv} [d_L \operatorname{Diag}(\mathbf{V}_L)]^{-1/2} \qquad \kappa_{011} = 0, \tag{25}$$

where the function Diag operates on a matrix to give a diagonal matrix, the elements of which are formed by the diagonal of the argument. After the change of variable the covariance matrix $\mathbf{V}_L$ simply becomes

$$\mathbf{W}_L = \mathbf{D}_L^{-1}(\mathbf{V}_L)_{\kappa_{011}=0}\mathbf{D}_L^{-1} \stackrel{\Delta}{\equiv} \begin{pmatrix} \mathbf{I} & \boldsymbol{\Gamma} \\ -\boldsymbol{\Gamma} & \mathbf{I} \end{pmatrix}, \tag{26}$$

where the submatrix $\boldsymbol{\Gamma}$ is given in Appendix C. In Appendix C the inverse of $\mathbf{W}_L$ is worked out formally in terms of the submatrices. The parameter d_L used in the first change of variable is defined as the square root of the determinant of the new covariance matrix $\mathbf{W}_L$:

$$d_L = \sqrt{|\mathbf{W}_L|} = \sqrt{|\mathbf{I} + \boldsymbol{\Gamma}^2|} = 1 - (\gamma^2_{\bar{1}10} + \gamma^2_{10\bar{1}}). \tag{27}$$

The squared variables in (27) are given in Appendix C, where the submatrix $\boldsymbol{\Gamma}$ is defined.

Similarly, the change of variable will affect the covariance matrix of short waves. Hence $\mathbf{V}_s$ becomes $\mathbf{W}_s$ as follows:

$$\mathbf{W}_s^{-1} = \frac{d_L}{d_s}\begin{pmatrix} \kappa_{020}\kappa_{02} & -\kappa_{11}\sqrt{\kappa_{020}\kappa_{002}} \\ -\kappa_{11}\sqrt{\kappa_{020}\kappa_{002}} & \kappa_{002}\kappa_{20} \end{pmatrix} \stackrel{\Delta}{\equiv} \begin{pmatrix} w_{20} & w_{11} \\ w_{11} & w_{02} \end{pmatrix}, \tag{28}$$

where the ws are helpful shorthand for the more complicated expressions of the corresponding terms.

Now this first change of variable can be explicitly introduced in the hydrodynamic bias of (20) to yield

$$\beta_H = \frac{\int \hat{T}(\mathbf{D}_L^{-1}\mathbf{u}_L)\cdot \hat{\mathbf{e}}_\zeta(\mathbf{D}_L^{-1}\mathbf{u}_L)\cdot \hat{\Sigma}\ \mathrm{e}^{-1/2\,{}^t\mathbf{u}_L\mathbf{W}_{Ls}^{-1}\mathbf{u}_L}\, d\mathbf{u}_L}{\int \hat{T}\ \mathrm{e}^{-1/2\,{}^t\mathbf{u}_L\mathbf{W}_{Ls}^{-1}\mathbf{u}_L}\, d\mathbf{u}_L} \tag{29}$$

in which the inverse of the new covariance matrices are combined into a single matrix

$$\mathbf{W}_{Ls}^{-1} = \mathbf{W}_L^{-1} + [\mathbf{W}_s^{-1}], \tag{30}$$

where the square bracket indicates a change of dimension. $\mathbf{W}_L^{-1}$ is 6×6, while $\mathbf{W}_s^{-1}$ is only 2×2. Therefore the sum in (30) is applied to the slope components only and not to their quadratures. The wide hat over T and Σ reflects the first change of variable to be included in the algebraic formulation below. After the first change of variable the hydrodynamic bias in (29) becomes an integral over a single 6-D Gaussian multiplied by a kernel function.

6.2. Second Change of Variable

The major difficulty in evaluating (29) analytically comes from the fact that the 6-D Gaussian is coupled in all its variables. In the following we will show a general approach to solving this problem. A second change of variable is now needed to decouple the 6-D Gaussian into six independent 1-D Gaussian integrals. To accomplish this goal, one decomposes the combined covariance matrix $\mathbf{W}_{Ls}^{-1}$ into a matrix multiplied by its transpose. The reason for that is

$${}^t\mathbf{u}_L\mathbf{W}_{Ls}^{-1}\mathbf{u}_L = {}^t\mathbf{u}_L{}^t\mathbf{S}\ \mathbf{S}\mathbf{u}_L = {}^t(\mathbf{S}\mathbf{u}_L)(\mathbf{S}\mathbf{u}_L), \tag{31}$$

where the new variable can be defined as $\mathbf{S}\mathbf{u}_L$. If the matrix $\mathbf{S}$ is not preconditioned, the decomposition will not be unique. However, if $\mathbf{S}$ is required to be triangular, then the decomposition is unique. This type of decomposition is well known in linear algebra as the Cholesky decomposition [e.g., *Golub and VanLoan*, 1996]. An alternative to the Cholesky decomposition in the present problem is to complete the squares "by hand" in the argument of the exponential. The Cholesky decomposition provides an automated process for decoupling multidimensional Gaussian distributions.

When this second change of variable is applied to (32), one gets

$$\beta_H = \sqrt{\kappa_{200}d_L}\,\frac{1}{(2\pi)^3} \cdot \int \hat{\hat{T}}(\mathbf{S}^{-1}\mathbf{u}_L)\cdot \hat{\mathbf{e}}_\zeta(\mathbf{S}^{-1}\mathbf{u}_L)\cdot (\mathbf{D}_L^{-1}\hat{\hat{\Sigma}})\mathrm{e}^{-1/2\,{}^t\mathbf{u}_L\mathbf{u}_L}\, d\mathbf{u}_L, \tag{32}$$

where the second wide hat over T and Σ reflects the second change of variable. The definition of the double wide hat operation can be spelled out as follows:

$$\hat{\hat{T}}(\mathbf{x}_L) \stackrel{\Delta}{\equiv} \hat{T}(\mathbf{D}_L^{-1'}\,\mathbf{x}_L) \stackrel{\Delta}{\equiv} T(\mathbf{D}_L^{-1'}\mathbf{S}^{-1'}\mathbf{x}_L) \tag{33a}$$

$$\hat{\hat{\Sigma}}(\mathbf{x}_L) \stackrel{\Delta}{\equiv} \hat{\Sigma}(\mathbf{D}_L^{-1'}\mathbf{x}_L) \stackrel{\Delta}{\equiv} \Sigma(\mathbf{D}_L^{-1'}\mathbf{S}^{-1'}\mathbf{x}_L), \tag{33b}$$

where the prime signs indicate that the operation is carried out only over the slope components of the regular signal and not on the quadrature moments.

6.3. Final Expression

After the second change of variable, the integral in (32) can be evaluated analytically since the multidimensional Gaussian is now uncoupled. The easiest way is to expand the integrand in powers of the moments. Every odd power of the moment variable vanishes and every even power will be replaced by the double factorial of the index minus one [see *Elfouhaily et al.*,

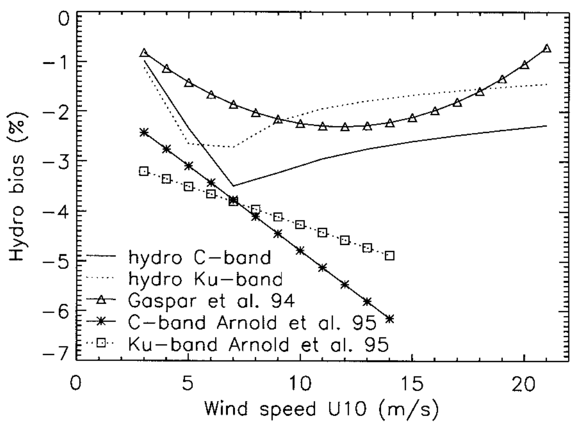

Figure 1. Numerical evaluation of the hydrodynamic bias β_H in (35) for wind-driven waves and where long and short waves are aligned. This simulated hydrodynamic bias is comparable with the current operational algorithm by *Gaspar et al.* [1994]. The frequency dependence is also in agreement with measurements by *Arnold et al.* [1995], especially when the tilt component [*Elfouhaily et al.*, 2000] is added.

2000]. A tedious algebraic manipulation yields this simple result:

$$\beta_H = \sqrt{\kappa_{200}}\left(\sqrt{\kappa_{200}}\Sigma_{\zeta} + \sqrt{\kappa_{020}}\ \gamma_{1\breve{1}0}\Sigma_{\breve{\zeta}_x} + \sqrt{\kappa_{002}}\ \gamma_{10\breve{1}}\Sigma_{\breve{\zeta}_y}\right), \qquad (34)$$

where indices on the vector Σ refer to corresponding components. An extra simplification can be carried out by replacing $\gamma_{1\breve{1}0}$ and $\gamma_{10\breve{1}}$ by their values as defined in Appendix C. As developed, the hydrodynamic bias expression becomes

$$\beta_H = \kappa_{200}\,\Sigma_{\zeta} + \kappa_{\breve{1}10}\,\Sigma_{\breve{\zeta}_x} + \kappa_{10\breve{1}}\Sigma_{\breve{\zeta}_y}. \qquad (35)$$

It is the sum of three terms. The first term is the elevation variance of long waves multiplied by the first element of the Σ vector in (18). The other two terms are similar but involve the cross moment between the elevation and the two quadratures of the slope components. The $\kappa_{1\breve{1}0}$ and $\kappa_{10\breve{1}}$ values being proportional to the orbital velocity variance of the long waves, our development explicitly indicates the fundamental role played by the straining of the short waves by the orbital motion of the long waves. The 6-D vector Σ is computed from the hydrodynamic transfer function. As defined, long-wave–short-wave interactions will impact the EM bias even though the original waves are linear. In other words, without the hydrodynamic modulation the EM bias would have been zero because of the absence of nonlinearities.

Figure 1 shows a numerical evaluation of the hydrodynamic bias β_H in (35) for the special case of a wind-driven sea where long and short waves are aligned. This example is not necessarily a common real-world occurrence. Nonetheless, our calculation provides reasonable agreement with empirical models. The model by *Gaspar et al.* [1994] is the current operational algorithm for TOPEX Ku band altimeter and is consistent with *Chelton* [1994]. It is worth noting that when the tilt component of the EM bias [*Elfouhaily et al.*, 2000] is added, our wind-driven simulation will be closer to the field experiment models by *Arnold et al.* [1995] for both Ku and C bands. The total EM bias will increase, in absolute value, by about 2%. It should also be noted that 1–3% on-orbit TOPEX EM bias levels are not necessarily universal since reported Poseidon and ERS Ku band altimeters can reach values as high as 5%. Experimental data, such as by *Walsh et al.* [1989], *Melville et al.* [1991], and *Arnold et al.* [1995], also exhibit these higher levels. New nonparametric studies propose that the EM bias for the TOPEX altimeter should be increased from around 2% to about 5% (P. Gaspar, personal communication, 1999).

Field experiment results should be utilized for safe frequency comparison of the EM bias since the dual-frequency TOPEX altimeter mixes information from both frequencies into its estimate of sea surface height. Our model's agreement in frequency dependence appears to improve on results achieved by *Rodriguez et al.* [1992] because now both the shape and magnitude of the wind dependence observed in the EM bias are reasonably captured. We note that the local minimum of the present illustration occurs at lower wind speeds than for the satellite or field observations. This feature, the general wind speed dependence of the model, and the absolute value of β_H will be assessed in forthcoming sensitivity studies.

In this simulation we used a 2-D spectrum for surface ocean waves [*Elfouhaily et al.*, 1997] that fulfills the desire expressed by *Rodriguez et al.* [1992, p. 2388] for a realistic spectral model. Not only did *Rodriguez et al.* [1992] use an unrealistic spectral model, but they also limited the problem to 1-D waves. In contrast to *Rodriguez et al.* [1992], we have derived, in (35), an analytic expression for the ensemble average EM bias instead of numerically averaged Monte-Carlo simulations. This is a considerable improvement since no complicated and repetitive numerical evaluations are needed. A single numerical run of (35) directly provides the statistical average of the EM bias. Another improvement on the work of *Rodriguez et al.* [1992] is that the hydrodynamic modulations are now accounted for in a fully 2-D context with extra modulation caused by heaving motions. The local acceleration is now included in the hydrodynamic modulations.

7. Nonlinear Modulating Waves

In the previous sections, both long- and short-wave statistics were taken to be Gaussian. In that case, waves of both scales were assumed to be a priori linear. A posteriori, however, modulated waves become nonlinear, and modulating waves remain linear. This induced nonlinearity in the modulated wave is responsible for the EM bias obtained in section 6. When long waves are themselves nonlinear, the hydrodynamic bias generated by the modulation will then comprise two kind of biases.

$$\beta_H = \beta_H^{\text{induced}} + \beta_H^{\text{inherent}}. \qquad (36)$$

The first term β_H^{induced} is identical to the previous hydrodynamic bias, which we call the induced hydrodynamic bias. The second term, however, depends on the nonlinearities of long waves as well as on the induced nonlinearity of short waves. This conjugation of the hydrodynamic modulation with tilting caused by nonlinear modulating waves we call the inherent hydrodynamic bias. In this final part of the paper we outline the analytical derivation of the hydrodynamic bias when the modulating waves are themselves nonlinear. A brief guidance is provided for the derivation of the EM bias when both short and long waves are inherently nonlinear in addition to the nonlinearity induced by the hydrodynamic modulation.

7.1. Generalized Perturbed Gaussian Model of Modulating Waves

The easiest way to approach the nonlinearity problem of long waves is to perturb slightly the multidimensional Gaussian distribution in a form similar to the Gram-Charlier expansion. The non-Gaussian PDF of the normalized moment vector can be formally expressed as

$$P_L^{nl}(\mathbf{v}_L) = \frac{1}{(2\pi)^3 d_L} \cdot e^{-1/2\, {}^t\mathbf{v}_L \mathbf{W}_L^{-1}\mathbf{v}_L} \left\{ 1 + \sum_{\Omega \geq 3} \sum_{p+q+r+}^{\check{p}+\check{q}+\check{r}=\Omega} \frac{\lambda_{pqr}^{\check{p}\check{q}\check{r}}}{p!q!r!\check{p}!\check{q}!\check{r}!} \mathrm{H}_{pqr}^{\check{p}\check{q}\check{r}}(\mathbf{v}_L) \right\}, \quad (37)$$

where $\lambda_{pqr}^{\check{p}\check{q}\check{r}}$ represents the joint nonlinear statistics of the 6-D moment vector. The functions $\mathrm{H}_{pqr}^{\check{p}\check{q}\check{r}}$ are generalized Hermite polynomials, which are defined by

$$\mathrm{H}_{pqr}^{\check{p}\check{q}\check{r}}(\mathbf{v}_L) = (-1)^{\Omega} P_L^{-1} \frac{\partial^{\Omega}}{\partial \eta^p \partial \eta_x^q \partial \eta_y^r \partial \check{\eta}^{\check{p}} \partial \check{\eta}_x^{\check{q}} \partial \check{\eta}_y^{\check{r}}} P_L(\mathbf{v}_L), \quad (38)$$

where Ω is the order of nonlinearity and the η variables represent the normalized random processes.

In our development the dimension of the workable space will always be higher than the order of nonlinearity. In other words, in most practical cases, Ω will always be smaller than 6. This means that each variable can be used as a tracer within a given order. Indeed, a tracer Hermite will suffice to describe all the Hermite polynomials that belong to the same order. In addition to this property, there is a relationship between the tracer Hermite from one order and the ones from previous orders. This recursion relation is found to be

$$\mathrm{H}_{100}^{\check{0}\check{0}\check{0}}(\mathbf{v}_L) = {}^t\hat{\mathbf{e}}_{\eta}\mathbf{W}_L^{-1}\mathbf{v}_L, \quad (39a)$$

$$\mathrm{H}_{110}^{\check{0}\check{0}\check{0}}(\mathbf{v}_L) = \mathrm{H}_{100}^{\check{0}\check{0}\check{0}}\mathrm{H}_{010}^{\check{0}\check{0}\check{0}} - \frac{\partial \mathrm{H}_{100}^{\check{0}\check{0}\check{0}}}{\partial \eta_x}, \quad (39b)$$

$$\mathrm{H}_{111}^{\check{0}\check{0}\check{0}}(\mathbf{v}_L) = \mathrm{H}_{110}^{\check{0}\check{0}\check{0}}\mathrm{H}_{001}^{\check{0}\check{0}\check{0}} - \frac{\partial \mathrm{H}_{110}^{\check{0}\check{0}\check{0}}}{\partial \eta_y}, \quad (39c)$$

$$\mathrm{H}_{111}^{\check{1}\check{0}\check{0}}(\mathbf{v}_L) = \mathrm{H}_{111}^{\check{0}\check{0}\check{0}}\mathrm{H}_{000}^{\check{1}\check{0}\check{0}} - \frac{\partial \mathrm{H}_{111}^{\check{0}\check{0}\check{0}}}{\partial \check{\eta}}, \quad (39d)$$

which is carried out up to the fourth (Kurtosis) order. More explicitly, the second- and third- (skewness) order expressions for the tracer Hermite polynomials are

$$\mathrm{H}_{110}^{\check{0}\check{0}\check{0}}(\mathbf{v}_L) = \mathrm{H}_{100}^{\check{0}\check{0}\check{0}}\mathrm{H}_{010}^{\check{0}\check{0}\check{0}} - {}^t\hat{\mathbf{e}}_{\eta}\mathbf{W}_L^{-1}\hat{\mathbf{e}}_{\eta_x} \stackrel{\Delta}{\equiv} \mathrm{H}_{100}^{\check{0}\check{0}\check{0}}\mathrm{H}_{010}^{\check{0}\check{0}\check{0}} - \mathrm{E}_{110}^{\check{0}\check{0}\check{0}} \quad (40a)$$

$$\mathrm{H}_{111}^{\check{0}\check{0}\check{0}}(\mathbf{v}_L) = \mathrm{H}_{100}^{\check{0}\check{0}\check{0}}\mathrm{H}_{010}^{\check{0}\check{0}\check{0}}\mathrm{H}_{001}^{\check{0}\check{0}\check{0}} - (\mathrm{E}_{110}^{\check{0}\check{0}\check{0}}\mathrm{H}_{001}^{\check{0}\check{0}\check{0}} + \mathrm{E}_{101}^{\check{0}\check{0}\check{0}}\mathrm{H}_{010}^{\check{0}\check{0}\check{0}} + \mathrm{E}_{011}^{\check{0}\check{0}\check{0}}\mathrm{H}_{100}^{\check{0}\check{0}\check{0}}), \quad (40b)$$

where the scalars E are the elements of the normalized covariance matrix of long waves ($\mathbf{W}_L^{-1}$). As stated before, the tracer Hermite in (40b) can be used to deduce all the third-order Hermite polynomials. For instance, if one needs the expression for this third-order Hermite $\mathrm{H}_{300}^{\check{0}\check{0}\check{0}}$, a quick look at (40b) provides the answer by simply changing the tracers to the real variables as follows:

$$\mathrm{H}_{300}^{\check{0}\check{0}\check{0}}(\mathbf{v}_L) = (\mathrm{H}_{100}^{\check{0}\check{0}\check{0}})^3 - 3\mathrm{E}_{200}^{\check{0}\check{0}\check{0}}\mathrm{H}_{100}^{\check{0}\check{0}\check{0}}, \quad (41)$$

where $\mathrm{E}_{200}^{\check{0}\check{0}\check{0}}$ is therefore the first diagonal element in $\mathbf{W}_L^{-1}$.

7.2. Inherent Hydrodynamic Bias

The hydrodynamic bias generated by this interaction with nonlinear long waves is then

$$\beta_H^{\text{inherent}} = \sqrt{\kappa_{200} d_L} \sum_{p+q+r+}^{\check{p}+\check{q}+\check{r}=4} \frac{\lambda_{pqr}^{\check{p}\check{q}\check{r}}}{p!q!r!\check{p}!\check{q}!\check{r}!} \mathrm{Q}_{pqr}^{\check{p}\check{q}\check{r}}, \quad (42)$$

where

$$\mathrm{Q}_{pqr}^{\check{p}\check{q}\check{r}} = \frac{1}{(2\pi)^3} \int \hat{T}(\mathbf{S}^{-1}\mathbf{u}_L) \cdot \hat{\mathbf{e}}_{\zeta}(\mathbf{S}^{-1}\mathbf{u}_L) \cdot (\mathbf{D}_L^{-1}\hat{\Sigma}) \widehat{\mathrm{H}}_{pqr}^{\check{p}\check{q}\check{r}} e^{-1/2\, {}^t\mathbf{u}_L\mathbf{u}_L}\, d\mathbf{u}_L \quad (43)$$

is obtained by introducing (37) into (32). The double wide hat reflects the successive change of variables as recapitulated here by

$${}_{pqr}^{\check{p}\check{q}\check{r}}(\mathbf{u}_L) \stackrel{\Delta}{\equiv} \hat{\mathrm{H}}_{pqr}^{\check{p}\check{q}\check{r}}(\mathbf{D}_L^{-1}\mathbf{u}_L) \stackrel{\Delta}{\equiv} \mathrm{H}_{pqr}^{\check{p}\check{q}\check{r}}(\mathbf{D}_L^{-1}\mathbf{S}^{-1}\mathbf{u}_L). \quad (44)$$

To illustrate the benefits of changing variables in the generalized Hermite, the tracer Hermite of first order after the change of variable simplifies to

$$\widehat{\mathrm{H}}_{100}^{\check{0}\check{0}\check{0}}(\mathbf{u}_L) = \mathrm{H}_{100}^{\check{0}\check{0}\check{0}}(\mathbf{D}_L^{-1}\mathbf{S}^{-1}\mathbf{u}_L) = \frac{1}{\sqrt{d_L}}\, {}^t(\mathbf{S}\hat{\mathbf{e}}_{\zeta})\mathbf{u}_L = \frac{\zeta}{d_L}. \quad (45)$$

In the $\mathrm{Q}_{pqr}^{\check{p}\check{q}\check{r}}$ integrals one can notice that the integrand consists of even powers in $\mathbf{u}_L$ if and only if the generalized Hermite is of even order. Hence the extra change in the tilting caused by the skewness order will not have any effect on the hydrodynamic bias. However, the kurtosis order will conjugate with the hydrodynamic modulation to give an enhanced modulation. Because of the overwhelming algebraic computation needed to find the final expression for $\beta_H^{\text{inherent}}$ in (42) for all the kurtosis orders, we provide the final result of a subelement of this fourth order. For instance, the final result of $\mathrm{Q}_{211}^{\check{0}\check{0}\check{0}}$, where the considered subelement is $\mathrm{H}_{200}^{\check{0}\check{0}\check{0}}\mathrm{H}_{010}^{\check{0}\check{0}\check{0}}\mathrm{H}_{011}^{\check{0}\check{0}\check{0}}$, is given by the following expression:

$$(\mathrm{Q}_{211}^{\check{0}\check{0}\check{0}})_{211} = \frac{\gamma_{\check{1}10}\gamma_{10\check{1}} + w_{11}}{d_L^2} \cdot \left[\left(\frac{\kappa_{\check{1}10}^2}{\kappa_{020}} + \frac{\kappa_{10\check{1}}^2}{\kappa_{002}} \right) \Sigma_{\zeta} + \kappa_{\check{1}10}\, \Sigma_{\check{\zeta}_x} + \kappa_{10\check{1}}\, \Sigma_{\check{\zeta}_y} \right], \quad (46)$$

which when introduced in (42), will reproduce a partial bias proportional to the kurtosis of the long modulating waves. The coefficient w_{11} in (46) is a clear manifestation of the nonlinear tilting in the hydrodynamic bias.

The skewness of long waves can enter the hydrodynamic bias only under the condition that short modulated waves are themselves inherently nonlinear. The nonlinearity in short waves induced by the hydrodynamic modulation is not sufficient to warrant the presence of the skewed tilting. However, if the short waves are skewed, then the skewness of the modulating waves will appear in the final expression of the hydrodynamic bias. The reason for this behavior becomes obvious when one traces the even and odd powers in the integrand of (43). Appendix D indicates the changes needed in the modulated quantities in order to bring the effect of the skewness in both short and long waves.

8. Conclusion

The present study clearly shows how both inherent and induced nonlinearities in long and short waves enter the electromagnetic bias problem. The inherent part is produced by the nonlinear nature of the waves before turning on the interaction between short and long waves. The induced component can exist even when both modulating and modulated waves are linear before allowing any hydrodynamic interaction between scales. This nonlinear process is then fundamentally different from the one that generates the tilt bias derived in previous work [see *Srokosz*, 1986; *Elfouhaily et al*., 2000]. Assuming that a surface wave spectrum can be effectively separated between faster moving modulating long waves and shorter steeper ones, the complete improved EM bias description is hence the sum of all components coming from the long waves' pure geometrical effects and induced hydrodynamic modulations.

As pioneered by *Alpers and Hasselmann* [1978], the modulation transfer function concept provides a simple means to model the variation of the short-wave spectrum in the presence of longer modulating waves. For the case of the radar altimeter the resulting modulation will lead to a correlation between the radar cross section and the surface wave elevation. Such a phenomenon will thus enter in the electromagnetic bias definition and can potentially add to the bias associated with the long-wave asymmetric profiles (so-called tilt bias).

In this study we rederived the hydrodynamic modulation transfer function from the wave action balance equation that includes both the orbital straining and a term carrying the effective acceleration of gravity. Higher derivatives of the modulating surface can be used within this formulation of the hydrodynamic MTF. However, measured spectra of long waves cannot guarantee sufficient accuracy for all derivatives of the surface elevation. Most surface spectra provide faithful estimates of the elevation moments. Fewer, however, can be used with confidence to predict both elevation and slope moments. For this reason the MTF was expanded in power of long wavenumbers and truncated to the linear order. This provides an explicit scale separation that must be consistent with the two-scale MTF concept. We further demonstrated that under this assumption and a GO approximation the expected radar cross section is conveniently expressed as a dot product between a modulation vector and a 6-D moment vector. The latter is constructed from the elevation and slope moments together with their quadratures. The modulation vector is related to the short-wave components. It is a function of the MTF, the proper relaxation rate, and the wind speed, friction velocity, and wave age, which could possibly enter in the formulation of the short-wave spectrum.

When the modulated radar cross section is used in the formulation of the EM bias, one faces the evaluation of a 6-D integral. The integrand of this multidimensional integral is nonlinear with the variable of integration. When the GO assumption is used, the kernel of this 6-D integral becomes a multidimensional Gaussian amenable for analytical evaluations. However, the multidimensional Gaussian involved is coupled in all its elements. We have shown one method for analytical evaluation using a linear change of variable based on the Cholesky decomposition.

After substantial algebraic manipulations, one arrives at a simple expression for the hydrodynamic bias by assuming, for simplicity, that both long and short waves are originally linear. Following our development, this first-order hydrodynamic bias is a sum of three terms. The first term is formed by the elevation variance and the elevation component of induced hydrodynamic modulation as expanded in powers of the long-scale wavenumber. The remaining two terms are functions of the orbital velocity variance of long waves as well as of the modulation by the elevation and the slope quadrature components. Although anticipated, this result explicitly shows the fundamental role played by the long-wave slope and orbital velocity components to interpret and to parameterize EM bias measurements.

A numerical simulation of this EM bias is shown in Figure 1. These results compare well with EM bias models based on observations. Our theory augments the numerical study conducted by *Rodriguez et al*. [1992] with the following features: 2-D realistic surface spectrum, 2-D extended hydrodynamic transfer function, and an analytic expression for the ensemble-averaged EM bias. These features ensure effectiveness while broadening the scope of the theory to real-world situations.

Higher-order statistics may also enter into the hydrodynamic bias. When present, the kurtosis of long waves can be conjugated with the induced nonlinearities of modulated waves to produce a nonlinear hydrodynamic bias. Further, the skewness of long waves should not impact the hydrodynamic bias unless the short waves are inherently nonlinear. In other words the skewness of long waves will conjugate with the skewness of short waves, for instance, to generate higher-order hydrodynamic biases.

In the next phase of this research effort we plan to examine our refined EM bias theory to assess its sensitivity to the value of critical input parameters such as the relaxation rate function, the assumed form of the long- and short-wave spectrum, and the explicit inclusion of nonlinearities. Such sensitivity studies along with comparisons with data from field experiments as well as on orbit satellites will provide estimates of the effect of these parameters on the computed EM bias and focus the design of future experimental campaigns.

Appendix A: Partial Derivatives of the Covariance Matrix

Under GO assumption for electromagnetic scattering a relative variation of the radar cross section yields the following expressions:

$$f_{20}(\mathbf{x}_L) = -\frac{1}{2}\frac{\kappa_{20}\kappa_{02}}{d_s} - \frac{1}{2}{}^t\mathbf{x}_L\Delta_{20}\mathbf{x}_L \tag{A1}$$

$$f_{11}(\mathbf{x}_L) = \frac{\kappa_{11}^2}{d_s} - \frac{1}{2}{}^t\mathbf{x}_L\Delta_{11}\mathbf{x}_L, \tag{A2}$$

where the delta functions are defined by

$$\Delta_{20} = \frac{\partial \mathbf{V}_s^{-1}}{\partial \ln \kappa_{02}} = \frac{1}{d_s^2}\begin{pmatrix} -\kappa_{02}\kappa_{02} & \kappa_{02}\kappa_{11} \\ \kappa_{02}\kappa_{11} & -\kappa_{11}\kappa_{11} \end{pmatrix} \tag{A3a}$$

$$\Delta_{11} = \frac{\partial \mathbf{V}_s^{-1}}{\partial \ln \kappa_{11}} = -\frac{1}{d_s^2}\begin{pmatrix} -2\kappa_{02}\kappa_{11} & \kappa_{20}\kappa_{02} + \kappa_{11}^2 \\ \kappa_{20}\kappa_{02} + \kappa_{11}^2 & -2\kappa_{20}\kappa_{11} \end{pmatrix}, \tag{A3b}$$

revealing a binomial dependence on the moment vector.

Appendix B: Gradient of the MTF

The gradient of the 2-D hydrodynamic MTF is

$$\nabla R(\mathbf{k}_L, \mathbf{k}_s) = (\mathbf{k}_L \cdot \mathbf{k}_s)(\mathbf{k}_L \cdot \mathbf{\Pi}_s)\nabla M_L^s + M_L^s(\mathbf{k}_L \cdot \mathbf{\Pi}_s)(c_s k_s + \nabla L_g) + M_L^s(\mathbf{k}_L \cdot \mathbf{k}_s)\mathbf{\Pi}_s, \quad \text{(B1)}$$

where

$$\nabla M_L^s = -\mu_s^2 \frac{c_L^2}{2c_s} \frac{1 + \mathrm{i}\left(\frac{\omega_L}{\mu_s} - \frac{\mu_s}{\omega_L}\right)}{(\omega_L^2 + \mu_s^2)^2} \frac{\mathbf{k}_L}{k_L} \quad \text{(B2a)}$$

$$\nabla L_g = -\frac{3}{4} c_L \mathbf{k}_L. \quad \text{(B2b)}$$

M_L^s carries the phase of the modulation because it is the only complex quantity in the MTF expression. L_g is an omnidirectional correction to the MTF due to the effective acceleration of gravity felt by short waves when riding on moving long waves.

Appendix C: Inverse of the Block Covariance

The submatrix $\underline{\Gamma}$ is defined by

$$\mathbf{\Gamma} = \begin{pmatrix} 0 & \frac{\kappa_{\bar{1}10}}{\sqrt{\kappa_{200}\kappa_{020}}} & \frac{\kappa_{101}}{\sqrt{\kappa_{200}\kappa_{002}}} \\ -\frac{\kappa_{\bar{1}10}}{\sqrt{\kappa_{200}\kappa_{020}}} & 0 & 0 \\ -\frac{\kappa_{101}}{\sqrt{\kappa_{200}\kappa_{002}}} & 0 & 0 \end{pmatrix} \stackrel{\Delta}{\equiv} \begin{pmatrix} 0 & \gamma_{\bar{1}10} & \gamma_{10\bar{1}} \\ =\gamma_{\bar{1}10} & 0 & 0 \\ -\gamma_{10\bar{1}} & 0 & 0 \end{pmatrix}, \quad \text{(C1)}$$

which yields to the formal inverse of the $\underline{\underline{W}}_L$ as follows:

$$\mathbf{W}_L^{-1} = d_L \begin{pmatrix} (\mathbf{I} + \mathbf{\Gamma}^2)^{-1} & -\mathbf{\Gamma}(\mathbf{I} + \mathbf{\Gamma}^2)^{-1} \\ \mathbf{\Gamma}(\mathbf{I} + \mathbf{\Gamma}^2)^{-1} & (\mathbf{I} + \mathbf{\Gamma}^2)^{-1} \end{pmatrix} = \begin{pmatrix} \mathbf{\Lambda} & -\mathbf{\Gamma} \\ \mathbf{\Gamma} & \mathbf{\Lambda} \end{pmatrix}, \quad \text{(C2)}$$

where the submatrix $\mathbf{\Lambda}$ is given by

$$\mathbf{\Lambda} \stackrel{\Delta}{\equiv} (\mathbf{I} + \mathbf{\Gamma}^2)^{-1} = \begin{pmatrix} 1 & 0 & 0 \\ 0 & 1 - \gamma_{10\bar{1}}^2 & \gamma_{\bar{1}10}\gamma_{10\bar{1}} \\ 0 & \gamma_{\bar{1}10}\gamma_{10\bar{1}} & 1 - \gamma_{\bar{1}10}^2 \end{pmatrix}. \quad \text{(C3)}$$

Appendix D: Nonlinear Short Waves

The skewed PDF of short waves can be written as a generalized Gram-Charlier expansion:

$$\sigma^o \propto P_s^{nl}(\mathbf{x}_L) = \frac{1}{\sqrt{d_s}} \mathrm{e}^{-1/2\, {}^t\mathbf{x}_L \mathbf{V}_s^{-1} \mathbf{x}_L} \left\{ 1 + \sum_{m+n=3} \frac{\lambda_{mn}}{m!n!} \mathrm{H}_{mn}(\mathbf{x}_L) \right\}, \quad \text{(D1)}$$

where $\mathbf{x}_L$ is a 2-D vector formed by the component of the slopes. The modulated radar cross section becomes

$$\frac{\delta\sigma^o}{\sigma^o} = \tilde{f}_{20} \frac{\delta\kappa_{20}}{\kappa_{20}} + \tilde{f}_{11} \frac{\delta\kappa_{11}}{\kappa_{11}} + \tilde{f}_{02} \frac{\delta\kappa_{02}}{\kappa_{02}} + \sum_{m+n=3} \mathrm{H}_{mn} \frac{\delta\lambda_{mn}}{m!n!}, \quad \text{(D2)}$$

where the tilde over the f functions indicates a change in the expression versus the linear case previously given in Appendix A. The changes are

$$\tilde{f}_{20}(\mathbf{x}_L) = -\frac{1}{2} \frac{\kappa_{20}\kappa_{02}}{d_s} - \frac{1}{2}\, {}^t\mathbf{x}_L \mathbf{\Delta}_{20} \mathbf{x}_L + \sum_{m+n=3} \frac{\lambda_{mn}}{m!n!} \frac{\partial \mathrm{H}_{mn}}{\partial \ln \kappa_{20}} \quad \text{(D3)}$$

$$\tilde{f}_{11}(\mathbf{x}_L) = \frac{\kappa_{11}^2}{d_s} - \frac{1}{2}\, {}^t\mathbf{x}_L \mathbf{\Delta}_{11} \mathbf{x}_L + \sum_{m+n=3} \frac{\lambda_{mn}}{m!n!} \frac{\partial \mathrm{H}_{mn}}{\partial \ln \kappa_{11}}. \quad \text{(D4)}$$

The modulated skewness parameters can be calculated in the following manner:

$$\delta\lambda_{mn} \stackrel{\Delta}{\equiv} \iint K_{mn}(\mathbf{k}_1, \mathbf{k}_2)\delta\Psi(\mathbf{k}_1)\delta\Psi(\mathbf{k}_2)\, d\mathbf{k}_1\, d\mathbf{k}_2 = \iint K_{mn}(\mathbf{k}_1, \mathbf{k}_2)\Psi(\mathbf{k}_1)\Psi(\mathbf{k}_2)(\mathbf{C}_{\mathbf{k}_1} \cdot \mathbf{u}_L) \cdot (\mathbf{C}_{\mathbf{k}_2} \cdot \mathbf{u}_L)\, d\mathbf{k}_1\, d\mathbf{k}_2, \quad \text{(D5)}$$

where $K_{mn}(\mathbf{k}_1, \mathbf{k}_2)$ is an assumed kernel function to be determined by the nature of the hydrodynamic interaction among long waves.

References

Alpers, W., and K. Hasselmann, The two-frequency microwave technique for measuring ocean wave spectra from an airplane or satellite, *Boundary Layer Meteorol.*, *13*, 215–230, 1978.

Arnold, D. V., W. K. Melville, R. H. Stewart, J. A. Kong, W. C. Keller, and E. Lamarre, Measurements of electromagnetic bias at Ku and C bands, *J. Geophys. Res.*, *100*, 969–980, 1995.

Barrick, D., Rough surface scattering based on the specular point theory, *IEEE Trans. Antennas Propag.*, *AP-16*, 449–454, 1968.

Chelton, D., The sea state bias in altimeter estimates of sea level from collinear analysis of TOPEX data, *J. Geophys. Res.*, *99*, 24,995–25,008, 1994.

Donelan, M., and W. Pierson, Radar scattering and equilibrium ranges in wind-generated waves with application to scatterometry, *J. Geophys. Res.*, *92*, 4971–5029, 1987.

Elfouhaily, T., B. Chapron, K. Katsaros, and D. Vandemark, A unified directional spectrum for long and short wind-driven waves, *J. Geophys. Res.*, *102*, 15,781–15,796, 1997.

Elfouhaily, T., D. R. Thompson, B. Chapron, and D. Vandemark, Improved electromagnetic bias theory, *J. Geophys. Res.*, *105*, 1299–1310, 2000.

Gaspar, P., F. Ogor, P.-Y. L. Traon, and O.-Z. Zanifé, Estimating the sea state bias of the TOPEX and Poseidon altimeters from crossover differences, *J. Geophys. Res.*, *99*, 24,981–24,994, 1994.

Golub, G. H., and C. F. VanLoan, *Matrix Computations*, *Johns Hopkins Studies in the Mathematical Sciences*, 3rd ed., 694 pp., Johns Hopkins Univ. Press, Baltimore, Md., 1996.

Kudryavtsev, V. N., The coupling of wind and internal waves: Modulation and friction mechanisms, *J. Fluid Mech.*, *278*, 33–62, 1994.

Liu, P. C., An evaluation of parameters for the theoretical distribution of periods and amplitudes of sea waves, *J. Geophys. Res.*, *81*, 3161–3162, 1976.

Longuet-Higgins, M. S., On the joint distribution of the periods and amplitudes of sea waves, *J. Geophys. Res.*, *80*, 2688–2694, 1975.

Melville, W. K., R. H. Stewart, W. C. Keller, J. A. Kong, D. V. Arnold, A. T. Jessup, M. R. Loewen, and A. M. Slinn, Measurements of electromagnetic bias in radar altimetry, *J. Geophys. Res.*, *96*, 4915–4924, 1991.

Phillips, O., Spectral and statistical properties of the equilibrium range in the wind-generated gravity waves, *J. Fluid Mech.*, *156*, 505–531, 1985.

Plant, W. J., A relationship between wind stress and wave slope, *J. Geophys. Res.*, *87*, 1961–1967, 1982.

Rodriguez, E., Y. Kim, and J. M. Martin, The effect of small-wave modulation on the electromagnetic bias, *J. Geophys. Res.*, *97*, 2379–2389, 1992.

Srokosz, M., On the joint distribution of surface elevation and slopes for a non-linear random sea, with an application to radar altimetry, *J. Geophys. Res.*, *91*, 995–1006, 1986.

Tayfun, M. A., On narrow-band representation of ocean waves, 1, Theory, *J. Geophys. Res.*, *91*, 7743–7752, 1986.

Walsh, E. J., F. C. Jackson, E. A. Uliana, and R. N. Swift, Observations of electromagnetic bias in radar altimeter sea surface measurements, *J. Geophys. Res.*, *94*, 14,575–14,584, 1989.

B. Chapron, Département d'Océanographie Spatiale, IFREMER, Centre de Brest, BP 70, 29280 Plouzané, France.

T. Elfouhaily and D. R. Thompson, Applied Physics Laboratory, The Johns Hopkins University, 11100 Johns Hopkins Road, Laurel, MD 20723–6099. (Elfouhaily@jhuapl.edu)

D. Vandemark, Laboratory for Hydrospheric Processes, NASA Goddard Space Flight Center, Wallops Island, VA 23337.

(Received October 5, 1999; revised October 13, 2000;
accepted October 19, 2000.)